JOURNAL OF APPLIED POLYMER SCIENCE VOL. 14, PP. 103–113 (1970)

Distribution of Internal Flaws in Acrylic Fibers

D. J. THORNE, *Composite Materials Research, Rolls-Royce Limited, Derby, England*

Synopsis

Optical microscopy has been used to illustrate various types of discontinuities, or flaws found within acrylic polymer fibers and to determine the distribution of such internal flaws along the length of the fiber. Flaws are comprised of particulate inclusions and voids. The internal flaw distributions approximate a Poisson type for point flaws, but significant variation is found in mean flaw concentrations from 0.03 to 2.3 flaws/mm. Both flaw concentration and flaw-free length distributions have been used to predict, for random selection of test lengths, the probability of avoiding a flaw with respect to gauge length (P versus L_g plots).

INTRODUCTION

Optical microscopy of commercially available polymer fibers has usually been limited to examination of fibers either in cross section to illustrate cross-sectional shape, diameter variation, and the presence of radial pores[1–4] or in transverse mode to assist identification.[5] Detailed examination of bright polymer fibers along the fiber length and perpendicular to the fiber axis discloses the presence of discontinuities, or flaws, within the fibers. These internal flaws, while not seriously affecting textile properties except in excessive concentrations,[6] represent contamination of the polymer structure and may influence tensile strength when brittle fracture is induced, for example by testing after heat treatment.[7]

In this present study various types of internal flaws have been observed and flaw distributions along the length of the fiber have been quantitatively determined in a wide selection of commercial acrylics. Dull fibers, intentionally impregnated with particulate pigments such as titanium dioxide to improve appearance or stability, have been excluded.

EXPERIMENTAL

Materials

Samples of bright acrylic fibers used in this study, available from world-wide sources[8] and representing products of ten commercial producers, are grouped geographically in Table I. The samples were received in the form of either tows or yarns composed of continuous fibers of fiber size less

TABLE I
Description of Acrylic Fiber Samples

Acrylic sample	Producer	Spinning		Fiber denier
		Method	Solvent	
1a	A	wet	inorganic	1.5
1b	A	wet	inorganic	1.5
1c	A	wet	inorganic	1.5
2	B	wet	organic	5
3	B	wet	organic	3
4	C	—	—	5
5	D	wet	organic	3
6	E	dry	organic	6
7	E	dry	organic	3
8	F	dry	organic	3
9	G	wet	inorganic	5
10	H	wet	inorganic	4.5
11	I	wet	inorganic	2
12	J	—	—	3

than 6 denier or 20 μm diameter and were retained free from undue atmospheric particulate contamination by enclosure in clean polythene sheet.

Prior to examination the samples usually required additional drawing to emphasize the presence of internal flaws. This was most readily achieved without contamination of fiber surface by stretching 50%–200% at 100°–150°C over 5–15 min in a stream of air filtered to a nominal 0.2 μm. Overstretching of the samples was avoided as this leads to the development of discontinuities in the optical properties along the fiber length and eventually to the introduction of stretch voids and then fracture.

Microscopic Method

Optical microscopy was used exclusively to examine internal flaws in the acrylic fibers. Stretched fibers were randomly selected and mounted parallel on microscope slides, immersed in cedar oil (n_D = 1.510) and then viewed in transmitted, polarized light at magnifications of ×200 to ×2000.

Internal flaws were distinguished from slight surface particulate contamination by careful focussing and by the characteristic elongation of internal flaws caused by the high degree of stretch given to the fibers prior to examination. Particles were accompanied by stretch cavities on either side but were distinguished from genuine voids by optical characteristics of refractive index, birefringence, or opacity.

For the quantitative determination of flaw distribution, 38-mm lengths of stretched fiber were continuously scanned and the numbers of internal flaws and distances between them (flaw-free lengths) were recorded. Measurable interflaw distances were limited at the high end to 38 mm and at the low end to 0.1 mm. Flaws occurring within 0.1 mm of each other were classed as

one flaw; this especially applied to the smallest particulate flaws which frequently occurred as strings of more than two particles separated by a distance of only a few μm. Occasional regions of fiber, up to 5 mm in length, which were virtually continuously flawed were recorded separately. Usually one determination covered 100–230 mm (6 fibers) but total lengths of stretched fiber up to 1700 mm (45 fibers) were necessary for the less flawed samples.

RESULTS AND DISCUSSION

Types of Internal Flaw

The various types of internal flaw observed in commercial acrylics are illustrated diagrammatically in Figure 1 and microscopically in Figure 2. The smaller particles (0.5–1.0 μm) appear almost opaque, are considered to be inorganic in composition, and are presumably incorporated by atmospheric contamination of fiber-spinning dope materials. There is an indication that acrylics wet-spun using an aqueous inorganic solvent are most heavily contaminated with this kind of particle; organic spinning solvents which have been distilled should be relatively free of such particulate contamination.

The larger particles (1–4 μm) with typical diconical stretch cavities have been observed previously[7] to melt on heating to around 200°C and are considered to be organic. Their optical properties vary from highly birefringent to poorly birefringent and in extreme cases appear as bridged dis-

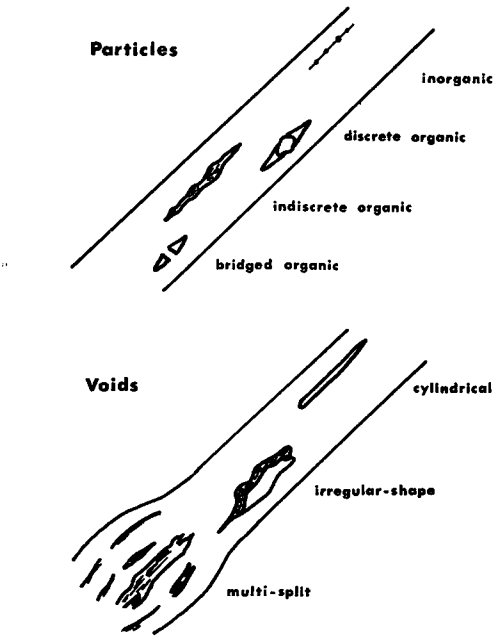

Fig. 1. Types of internal flaw in acrylic polymer fibers.

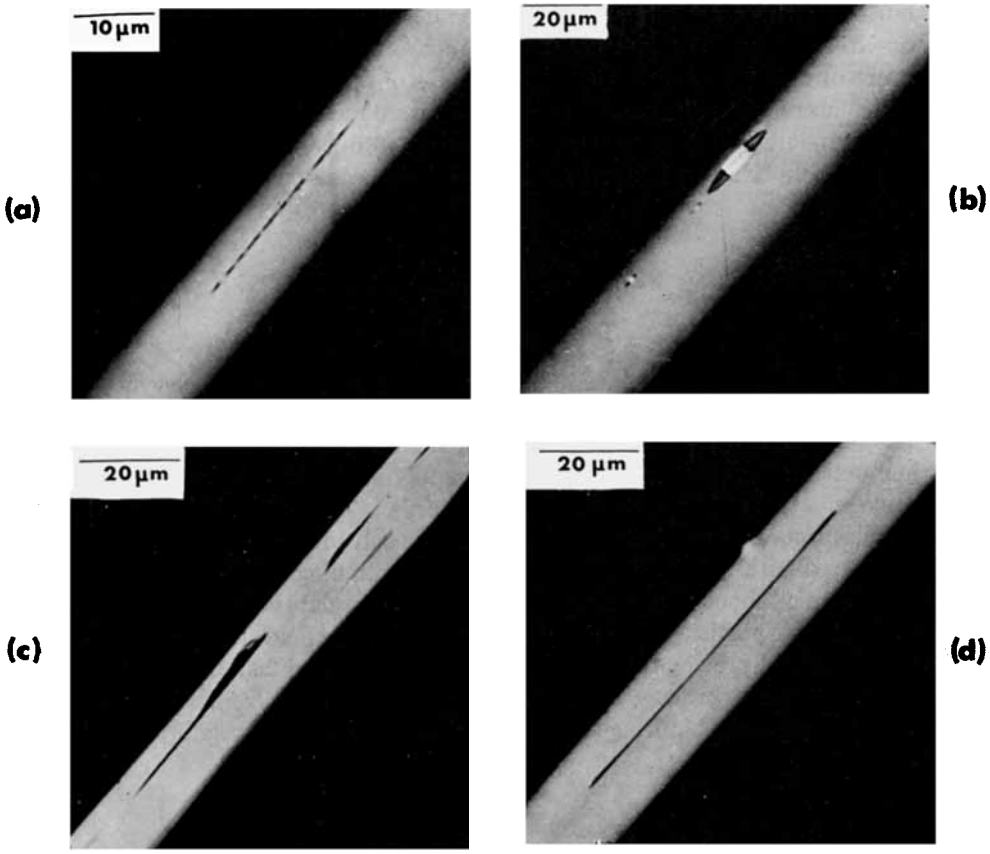

Fig. 2. Examples of internal flaws in acrylic polymer fibers: (a) inorganic particles; (b) organic particles; (c) irregular-shaped voids; (d) cylindrical void.

continuities in the polymer. These particles have been observed mainly in wet-spun acrylics.

Different types of voids can be differentiated only by their geometrical shape and size. The more usual cylindrical voids are thought to be caused by gases dissolved in the fiber-spinning dope whereas the irregular-shaped voids are thought more likely to be caused by irregular flow at the spinneret orifice (extrusion cavities) or by too rapid coagulation of the polymer.

Flaw Concentration and Flaw-Free Length

Determined mean flaw concentrations and mean flaw-free lengths are given in Table II. All results given in this paper refer to the as-received fiber, i.e., compensation has been made for the degree of stretch applied prior to examination.

It is immediately plain that a wide variation in the internal flaw concentration occurs between different acrylics. The higher concentrations of flaws

TABLE II
Mean Flaw Concentration and Flaw-Free Length Determinations

Acrylic sample	Fiber length examined, mm	Mean flaw concentration, mm^{-1}	Mean flaw-free length, mm
1a	110	2.32	0.5
1b	345	0.98	1.0
1c	300	0.57	1.7
2	100	2.10	0.5
3	130	1.20	0.8
4	260	0.32	3.4
5	300	0.26	3.1
6	840	0.11	>8
7	1660	0.03	>25
8	115	1.48	0.7
9	230	0.39	2.6
10	150	0.17	>5
11	205	0.27	3.5
12	705	0.09	>8

were generally due to increased numbers of both particles and voids, with a few exceptions; for example, in samples 2 and 3, voids overwhelmingly predominated and in the less flawed sample 10, voids were exclusively observed. Mean flaw-free lengths, of course, approximate to recriprocal mean flaw concentrations. With the cleaner fibers the number of flaw-free lengths actually observed becomes very low since a complete flaw-free length requires both an initial flaw and a terminal flaw within the scanned specimen length. Mean flaw concentration is therefore preferred for initial comparison of fibers.

Distribution of Flaws

Typical flaw concentration distributions are given in Figure 3. A Poisson-type distribution of point flaws is indicated, having the characteristic dependence on only one variable, the mean flaw concentration:

$$P = 1 - e^{-a}\left[1 + \frac{a}{1!} + \frac{a}{2!} + \cdots\cdots \frac{a^{c-1}}{(c-1)!}\right]$$

where P is the probability that an event will occur at least c times in a large group of trials where the average number of occurrences, (i.e., mean flaw concentration) is a.

Comparison of Poisson distribution predictions from the mean flaw concentrations with experimental results is therefore included in Figure 3. Reasonable agreement was generally found, the most serious deviation occurring with sample 12. It is concluded that for the majority of fiber samples the flaw distribution approximates a Poisson type.

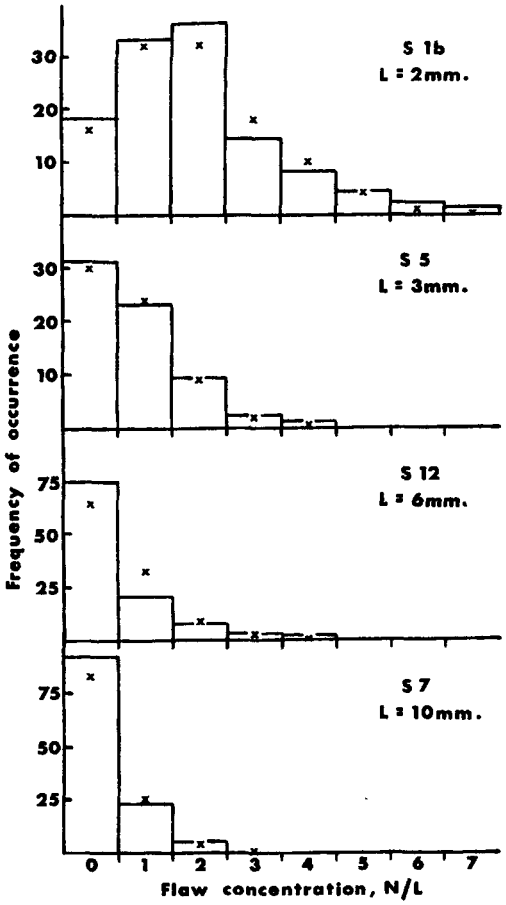

Fig. 3. Internal flaw concentration distributions in acrylic fibers and Poisson points predicted from means (see Table II).

Typical distributions of flaw-free lengths are given in Figure 4. These distributions give an immediate idea of the fiber lengths which can be obtained without a flaw in them.

Probability of Avoiding a Flaw

Fiber (or wire) tensile strength versus gauge length effects[9–12] can be used to predict the average frequency of flaw occurrence[12,13] on the assumption that discrete flaws are responsible for premature failure and, consequently, for decreased strength. In reverse, the probability of obtaining or avoiding a flaw within randomly selected gauge lengths could be a useful intermediate expression for relating flaw distribution to fiber tensile strength properties. In practice the main desire is to achieve high strength by avoiding serious flaws. The distribution of internal flaws in acrylic fibers may

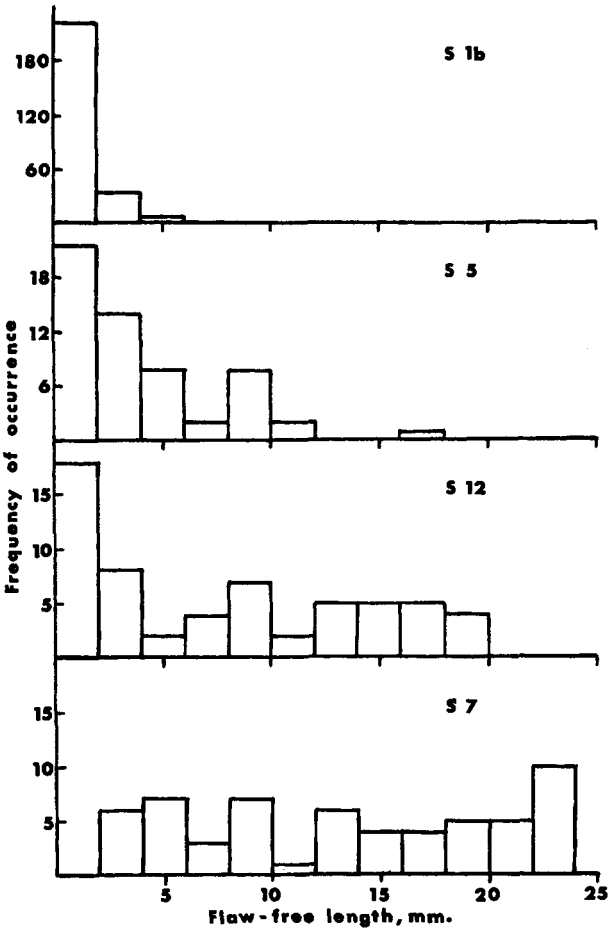

Fig. 4. Internal flaw-free length distributions in acrylic fibers.

therefore be reexpressed as the probability P of avoiding a flaw with respect to gauge length L_g.

Assuming that the internal flaw concentrations fit a Poisson distribution, P versus L_g plots can be readily prepared from standard Poisson probability curves (or from $P = e^{-a}$) using the mean flaw concentration values of Table II. This has been done in Figure 5 over the L_g range of 0–18 mm.

The Poisson prediction treats all flaws as point flaws. It cannot include those regions, observed in a few of the samples, which were continuously flawed, nor treat the flaws as having finite lengths. An empirical approach based on the flaw-free length distribution overcomes these difficulties.

In any flaw-free length l between two flaws, the effective length over which unflawed gauge lengths can be selected is given by $l - L_g$. The proportion p which can give unflawed gauge lengths is then given by

$$p = 1 - L_g/l. \tag{1}$$

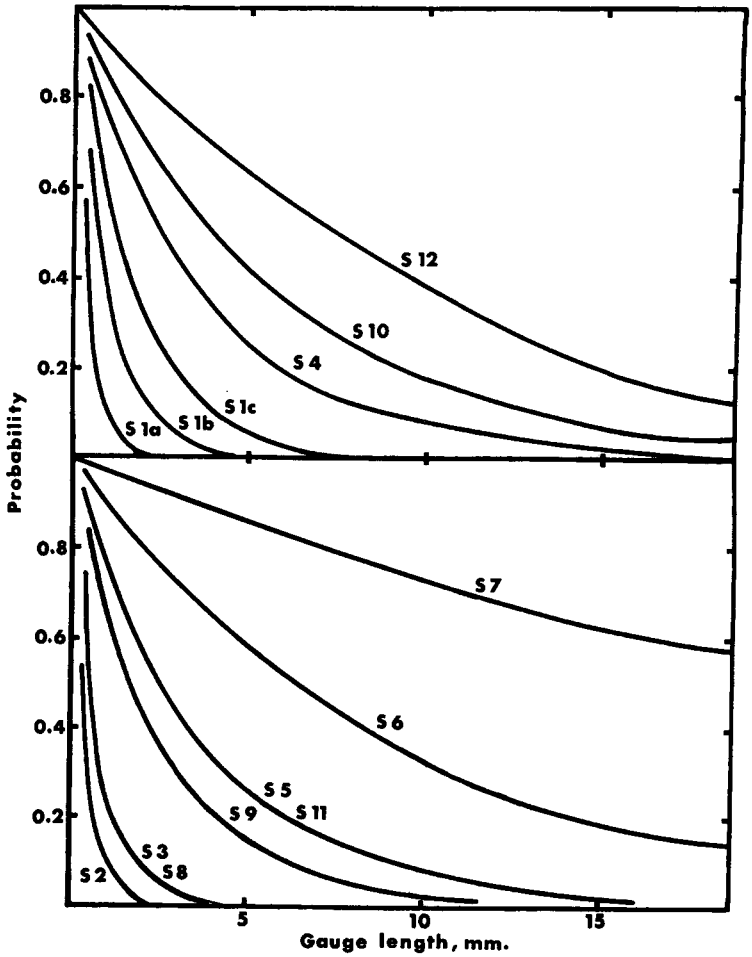

Fig. 5. Probability of avoiding internal flaw versus fiber gauge length. Poisson prediction from mean flaw concentrations (see Table II).

For a distribution of flaw-free lengths, each length will have an associated frequency n and an associated proportion p which can give unflawed gauge lengths. The expected number of unflawed gauge lengths for all values of $l > L_g$ (i.e., l', n', p') is then

$$1/L_g \sum l'n'p'$$

whereas the expected number of gauge lengths from the total length of fiber examined is

$$1/L_g \sum ln.$$

The probability of selecting unflawed gauge lengths is therefore given by

$$P = \frac{1/L_g \sum l'n'p'}{1/L_g \sum ln}.$$

Substituting for p' using eq. (1),

$$P = \frac{\sum|n'l' - n'L_g|}{\sum ln}. \tag{2}$$

Alternatively, eq. (2) may be written

$$P = \frac{L' - N'L_g}{L} \tag{3}$$

where L' is total length of all flaw-free lengths where $l > L_g$, N' is total number of all flaw-free lengths where $l > L_g$, and L is total length of fiber examined.

The empirical eq. (3) can accommodate lengths of fiber noted to be continuously flawed, can illustrate the effect of flaw length on the P versus L_g plot, and is applicable where deviation from a Poisson-type distribution of flaws occurs. Comparisons illustrating the effects of these variations are given in Figures 6 to 8.

Two fiber samples in which continuously flawed regions were found to account for 10%–12% of the total length examined are selected in Figure 6. The effect of including these regions in calculating the P versus L_g relation from the empirical eq. (3) is seen to be significant in the midprobability range. It is concluded that in the acrylic samples in which continuously flawed regions accounted for only up to a few per cent of the total length examined the effect is small and is adequately compensated for by the empirical approach. It must be stressed, however, that inclusion of the multiple flaws in these continuously flawed regions in determining mean flaw concentrations is not recommended.

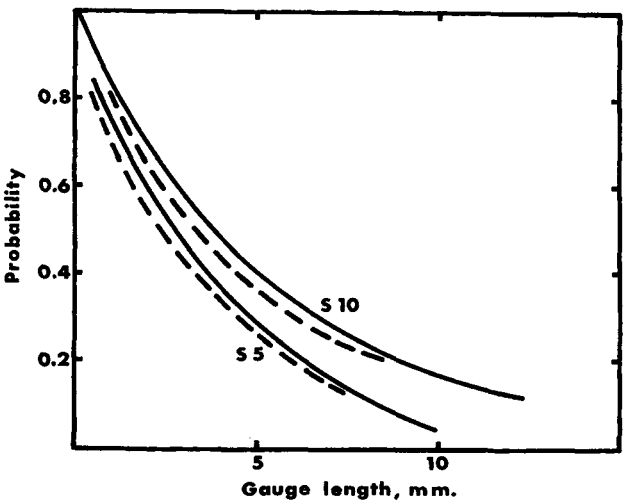

Fig. 6. Effect of including continuously flawed regions on P versus L_g curve, using empirical equation: (———) exclusion; (– – – –) inclusion.

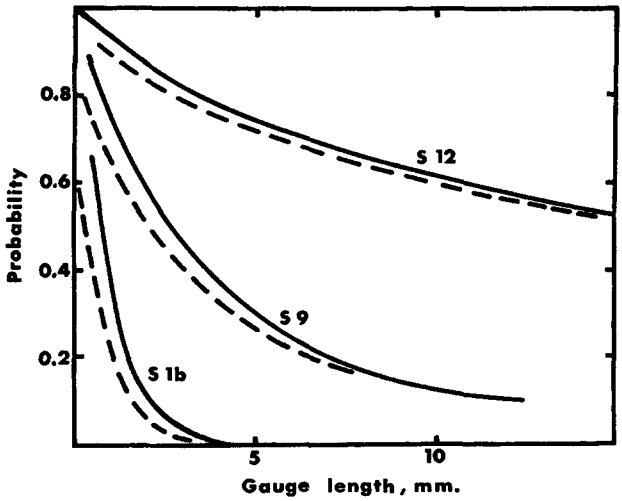

Fig. 7. Effect of including arbitrary flaw length on P versus L_g curve using empirical equation: (———) exclusion; (– – – –) inclusion.

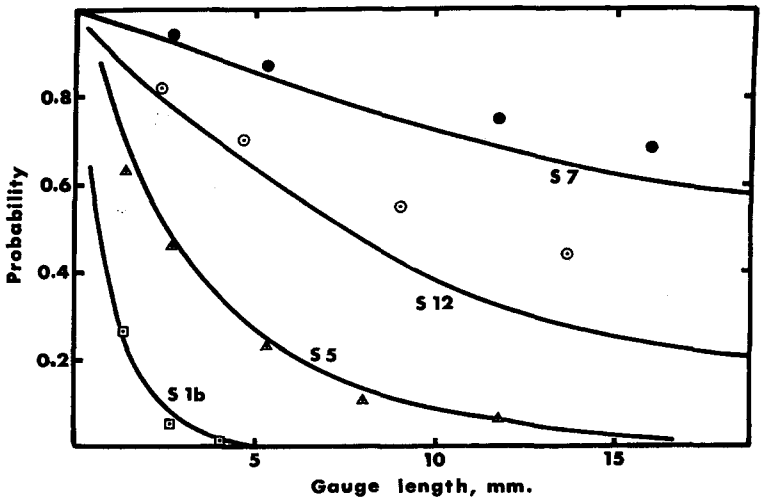

Fig. 8. Comparison of P versus L_g Poisson predicted curves and empirical equation points.

The effect of treating all flaws as having finite lengths is illustrated in Figure 7, in which an arbitrary flaw length of 0.5 mm has been used. In practice, however, average flaw lengths, excluding the continuously flawed regions, were found to be less than 0.05 mm. It is concluded therefore, that the effect of flaw length on the P versus L_g relation can be ignored.

As illustrated in Figure 8, the effect of deviation from a Poisson distribution of internal flaws on the P versus L_g relation can be more serious. For fiber samples 1b and 5, in which flaw concentrations were shown to follow closely a Poisson distribution (Fig. 3), the agreement between Poisson and

empirical equation predictions is good. For samples 6 and 12, in which flaw concentrations were indicted to deviate slightly from a Poisson distribution (Fig. 3), underestimation of P using the Poisson prediction is shown. Sample 12 represented the most serious deviation from a Poisson distribution of flaws. It is concluded that where deviation from a Poisson distribution of flaws occurs the empirical eq. (3) may be used to give a better estimate of the probability of avoiding an internal flaw with respect to gauge length. In practice, however, the flaw-free length distribution and therefore the empirical equation are limited by the maximum length of fiber that can be continuously scanned.

CONCLUSIONS

Microscopic examination along the length of commercial acrylic fibers has allowed the classification of various types of internal flaw, comprised of particulate inclusions and voids.

The distribution of internal flaws has been determined and is found to approximate a Poisson-type distribution, with wide variation from acrylic to acrylic in the mean flaw concentration over the range 0.03–2.3 flaws/mm.

Both flaw concentration and flaw-free length distributions have been used to predict the probability P of avoiding an internal flaw with respect to gauge length L_g, in the first case using a Poisson prediction from the mean flaw concentration and in the second case using the empirical equation

$$P = \frac{L' - N'L_g}{L} \tag{3}$$

The P versus L_g plots have been used to compare the various acrylic fiber samples and to illustrate the small effects of flaw length and the more serious effects of deviation from Poisson-type flaw distribution. In cases where deviation from Poisson distribution occurs, the empirical equation is more applicable.

References

1. H. R. Mauersberger, *Textile Fibers*, Wiley, New York, 1954.
2. J. P. Knudsen, *Text. Res. J.*, **33**, 13 (1963).
3. M. S. Mezhirov and E. A Pakshver, *Khim. Volokna*, **3**, 13 (1968).
4. H. Kawakami, N. Mori, and A. Miyoshi, *Sen-i Gakkaishi*, **23**, 533 (1967).
5. V. Nurzia, *Rass. Chim.*, **18**, 13 (1966).
6. I. Hedlund, S. Dunbrant, and K. Wilson, *Svensk Papperstidn.*, **21**, 241 (1968).
7. J. W. Johnson, *ACS Polymer Reprints*, **9**, 1316 (1968).
8. R. E. Sanders, *Chem. Process Eng.*, **49**, 100 (1968).
9. R. Meridith, *J. Text. Inst.*, **43**, 755 (1952).
10. G. K. Schmitz and A. G. Metcalfe, *Mater. Res Standards*, **7**, 146 (1967).
11. R. Moreton, *Fibre Sci Tech.*, **1**, 23 (1969).
12. K.. E. Puttick and M. W. Thring, *J. Iron Steel Inst.*, **172**, 56 (1952).
13. W. E. Morton and J. W. S. Hearle, *Physical Properties of Textile Fibers*, Butterworths, London, 1962.

Received May 12, 1969
Revised August 11, 1969